Simulation of Microwave Heating of a Composite Part in an Oven Cavity

Hermine Tertrais[1, a)], Ruben Ibanez[2,b)], Anaïs Barasinski[1, c)], Chady Ghnatios[3, d)] and Francisco Chinesta [2, e)]

[1]GeM-Ecole Centrale Nantes, 1 Rue de la Noë, 44321 Nantes, France
[2]ICI-Ecole Centrale Nantes, 1 Rue de la Noë, 44321 Nantes, France
[3]Notre Dame University-Louaize, Zouk Mosbeh, Lebanon

[a)] Corresponding author: hermine.tertrais@ec-nantes.fr
[b)]ruben.ibanez-pinillo@eleves.ec-nantes.fr
[c)]anais.barasinski@ec-nantes.fr
[d)]cghnatios@ndu.edu.lb
[e)]francisco.chinesta@ec-nantes.fr

Abstract. Microwave (MW) technology relies on volumetric heating. Thermal energy is transferred to the material that can absorb it at specific frequencies. In this paper, a coupled thermic and electromagnetic model is proposed in order to simulate the emerging process of microwave heating for composite materials. Solving the problem in a laminated composite material requires a high degree of discretization in the thickness direction which is made possible by introducing the in-plane-out-of-plane decomposition approach using the Proper Generalized Decomposition (PGD).

INTRODUCTION

Composites parts tend to represent an increasing volume of production in transport industry (aeronautic and automotive). This is due to their combination of high mechanical properties and low mass. However, one aspect is still a disadvantage: their long cycle time.

Conventional processing methods for producing polymer composite parts usually involve the application of heat to the material by convection heating of the tool and composite in an oven (pressurized/non-pressurized), or conductive heating of mold/platens through heating elements. Conversely to these traditional heating methods which depend on surface heat transfer, microwave (MW) technology relies on volumetric heating. Thermal energy is transferred through electromagnetic fields to materials that can absorb it at specific frequencies.

Volumetric heating enables better process temperature control [1] and less overall energy use, which can results in shorter processing cycles. The energy efficiency of the process is maximized as the volumetric heating occurs directly in the part to be processed, and no energy is wasted by heating the surrounding air or tool. These virtues of the MW technology have attracted interest in developing the method and adopting it for the production of thermoset as well as thermoplastic composite materials.

Substantial time and energy benefits have been reported [2, 3]. The shorter cycle is possible as the microwave oven requires minimal ramp-up to set point temperature and the process has less tooling-driven thermal lag. Further, when the oven shuts off, there is no cool-down of the oven itself. Furthermore, comparable mechanical properties are shown between parts made with the MW technology and parts made with a traditional curing system (autoclave in the case of [4]). The main drawback of this technology today is that the complex physics involved in the conversion of electromagnetic energy to thermal energy (heating) is not entirely understood and controlled.

The objective of this work is to model the interactions of the MW field with the composite material (Glass Fiber Reinforced Polymer or GFRP) and to describe how the local heat transfer mechanisms contribute to the overall heating of the produced part.

The main challenge concerns the high-resolution description of the electromagnetic and thermal fields in a composite laminate, that involve plies whose characteristic in-plane dimension is order of magnitude higher than the ones related to the thickness (typical aspect ratio are of tens of thousands). In that situation the use of in-plane-out-of-plane separated representations within the Proper Generalized Decomposition –PGD- framework seems an appealing and valuable route for solving 3D models, very rich in both, the in-plane and the out-of-plane directions, while ensuring a computational complexity of standard 2D models [5-8].

DESRIPTION OF THE PROCESS

As depicted on **FIGURE 1a.**, the oven cavity has a hexagonal shape, as for the Hephaïstos© oven. Microwaves are produced by twelve magnetrons placed around the cavity with a characteristic frequency of 2.45 GHz. The mold and the composite part are positioned on a metallic bench in the oven. The mold is composed of a material transparent to MW but coated in its interior surface by an absorbent layer.

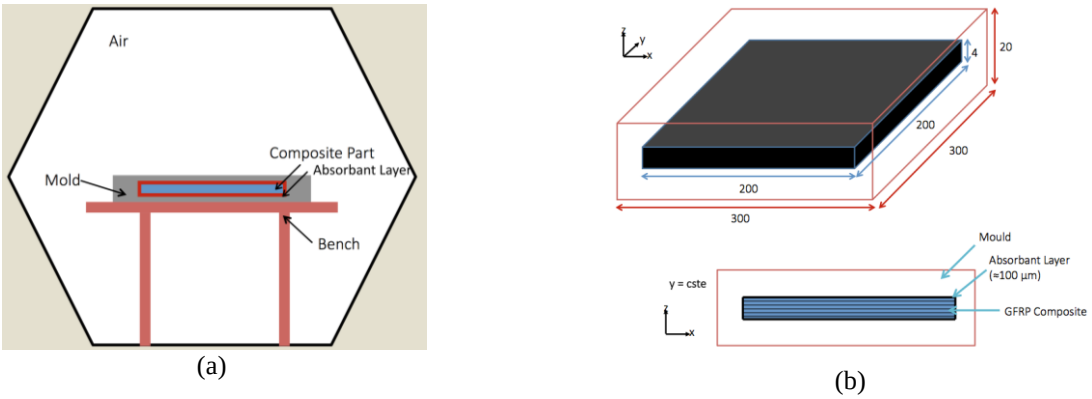

(a) (b)

FIGURE 1. Schematic representation of the process (a) and zoom of the mold and composite part with its characteristic dimensions in mm (b)

MODELLING THE MICROWAVE HEATING

Electromagnetic Model

A coupled electromagnetic and thermal model is proposed in order to simulate the emerging process of microwave heating for composite materials. The physical models for electromagnetics consist of the well-known Maxwell equations, which after some manipulations and assuming a harmonic electric field, are reduced to:

$$\nabla \times \frac{1}{\mu} \nabla \times \boldsymbol{E} = \gamma^2 \boldsymbol{E} \quad \text{with} \quad \gamma^2 = i\omega(\sigma + i\omega\varepsilon) \quad \text{in } \Omega \subset \mathbb{R}^3 \tag{1}$$

$$\boldsymbol{n} \times \boldsymbol{E} = \boldsymbol{E^t} \quad \text{in } \partial\Omega \tag{2}$$

where μ, ε and σ and respectively the permeability, the permittivity and the electrical conductivity, all three of them depending on the considered material and $\omega = 2\pi f$ with f the frequency. $\boldsymbol{n}$ refers to the unit outwards vector defined on the domain boundary and $\boldsymbol{E^t}$ is the prescribed electric field (assumed known) on the domain boundary.

The weak form is obtained by multiplying (1) by the conjugate test function $\overline{\boldsymbol{E}}^*$and by integrating by parts:

$$\int_\Omega \frac{1}{\mu}(\nabla \times \boldsymbol{E}) \cdot (\nabla \times \overline{\boldsymbol{E}}^*) d\Omega - \int_\Omega \gamma^2 \boldsymbol{E} \cdot \overline{\boldsymbol{E}}^* \, d\Omega - \int_{\partial\Omega} (\nabla \times \boldsymbol{E}) \cdot (\mathbf{n} \times \overline{\boldsymbol{E}}^*) d\Gamma = 0 \tag{3}$$

In (3), the integral on the boundary can be simplified if the test function verifies $\boldsymbol{n} \times \overline{\boldsymbol{E}}^* = 0$ i.e. where we have enforced $\boldsymbol{n} \times \boldsymbol{E}$. For simplicity, we consider that Dirichlet boundary conditions (BC) are applied on the whole domain boundary, therefore the boundary integral can be removed from (3). However, it is known [9] that this version of the weak form produces spurious solutions as even if (1) ensures the verification of the Gauss equation $\nabla \cdot (\varepsilon \boldsymbol{E}) = 0$, its discrete version after approximating the different fields implied in the weak form does not ensure the fulfillment of the Gauss equation. Therefore, a regularization is needed to avoid spurious solutions. The regularized form is then:

$$\nabla \times \frac{1}{\mu} \nabla \times \boldsymbol{E} \; - \bar{\varepsilon} \nabla \left(\frac{1}{\bar{\varepsilon} \varepsilon \mu} \nabla \cdot (\varepsilon \boldsymbol{E}) \right) = \gamma^2 \boldsymbol{E} \tag{4}$$

whose associated weak form (with Dirichlet BC applying on the whole domain boundary) is:

$$\int_\Omega \frac{1}{\mu} (\nabla \times \boldsymbol{E}) \cdot (\nabla \times \overline{\boldsymbol{E}}^*) d\Omega - \int_\Omega \gamma^2 \boldsymbol{E} \cdot \overline{\boldsymbol{E}}^* \, d\Omega + \int_\Omega \frac{1}{\bar{\varepsilon} \varepsilon \mu} \left(\nabla \cdot (\varepsilon \boldsymbol{E}) \right) \left(\nabla \cdot (\varepsilon \overline{\boldsymbol{E}}^*) \right) d\Omega + \int_{\partial\Omega} \frac{1}{\bar{\varepsilon} \varepsilon \mu} \left(\nabla \cdot (\varepsilon \boldsymbol{E}) \right) \cdot (\mathbf{n} \cdot (\bar{\varepsilon} \overline{\boldsymbol{E}}^*)) d\Gamma = 0 \tag{5}$$

In-plane-out-of-plane Separated Representation

As the composite part considered in the process is a plate, its characteristic in-plane dimension is orders of magnitude higher than the ones related to the thickness as shown on **FIGURE 1b**. In that situation, the use of the in-plane-out-of-plane separated representation within the Proper Generalized Decomposition (PGD) framework allows writing the electric field in the 3D separated form:

$$\boldsymbol{E}(x, y, z) \approx \sum_{i=1}^{N} \boldsymbol{X_i}(x, y) \circ \boldsymbol{Z_i}(z) \tag{6}$$

where the bullet $\circ$ denotes the Hadamar product. Thus, the electric field is expressed as a finite sum of functional couples involving a function depending on the in-plane coordinates (x,y) and the other involving the coordinate related to the thickness (z). Thus, the 3D solution is obtained from a number (in the order of N) of 2D problems involving the in-plane coordinates and the same number of 1D problems involving the thickness.

Such a separated representation seems an appealing and valuable route for solving 3D models, very rich in both, the in-plane and the out-of-plane directions, while ensuring a computational complexity of standard 2D models [5]. This separated representation is especially interesting for addressing domains in which at least one of its characteristic dimensions is much smaller than the others, and the solution exhibits significant richness in the thickness direction implying the necessity of using a fine enough representation (mesh) to capture the transmission conditions at the ply interfaces. When using standard mesh-based discretization the use of a fine mesh in the thickness direction within a 3D discretization usually implies extremely fine meshes in the whole domain, involving a prohibitive number of degrees of freedom. The use of separated representations makes independent the in-plane and the thickness approximations and the use of different discretization techniques for solving the associated problems related to the in-plane and the thickness coordinates is possible.

The solution procedure proceeds by calculating at each enrichment iteration a new functional couple. Because the calculating of two unknown functions defines a nonlinear problem, a second iteration loop must be considered. By assuming the function depending in the z-coordinate known (randomly chosen when starting the nonlinear loop) the function depending in the in-plane coordinates is calculated by solving the associated 2D problem. Then, from it, the function depending on the z-coordinate is updated and so on. As soon as the iteration converges, the next functional couple is searched. The enrichment stops as soon as the residual associated to the solution becomes small enough, which we assumed occurs after adding N functional couples. All the details can be found in [8].

Interface Conditions

The electric field propagation at interfaces is ruled by the following equation in a free-charge space:

$$(\varepsilon_1 \boldsymbol{E}_1 - \varepsilon_2 \boldsymbol{E}_2) \cdot \boldsymbol{n} = 0 \quad (7)$$

$$(\boldsymbol{E}_1 - \boldsymbol{E}_2) \times \boldsymbol{n} = 0 \quad (8)$$

These interfaces conditions highlight the continuity of the electric field for the tangential components and the discontinuity of the normal component. In the case we are considering, it is assumed that the only interfaces are along the thickness (z coordinate), thus we use a standard continuous nodal approximation of fields E_x and E_y. For the E_z component, we have to consider the fact that it is continuous in the plane but discontinuous at interfaces where the field jump is:

$$\varepsilon_1 E_z(z^-) = \varepsilon_2 E_z(z^+) \quad (9)$$

where $E_z(z^-)$ and $E_z(z^+)$ are the electric field at both sides of the interface. In order to enforce the discontinuity, the nodes at interfaces in the out-of-plane mesh used to approximate the z-component of $\boldsymbol{Z_i}$ functions, are duplicated, each one being used to approximate the solution at one side of the interface.

Thermal Model

From the electromagnetic solution, the thermal source term Q can be determined and the thermal model defined and solved. The heat conduction model inside the laminate allows calculating the temperature field at each position and time $T(x, y, z, t)$ by solving the heat equation:

$$\rho C_p \frac{\partial T}{\partial t} = \nabla \cdot (\boldsymbol{K} \cdot \nabla T) + Q(x, y, z, t) \quad (10)$$

where $\boldsymbol{K}$ represents the thermal conductivity tensor defined at the ply level and which in the case of unidirectional reinforcement or fabrics becomes anisotropic justifying its tensorial character.

Again, the too different in-plane and thickness characteristic lengths, motivates the use of a separated representation of the temperature field, which now writes:

$$T(x, y, z, t) \approx \sum_{i=1}^{M} X_i(x, y) Z_i(z) \theta_i(t) \quad (11)$$

and allows calculating a fully 3D transient solutions while keeping the computational complexity characteristic of 2D solutions (the ones involved in the calculations of function depending on the in-plane coordinates (x,y)). In the case of the parabolic heat equation, the separated representation at the heart of the PGD method allows the time integration in a non-incremental way, that is, the whole temperature history is computed simultaneously. This ability allows impressive CPU time savings, of many orders of magnitude.

TEST CASE

Some simple test cases are shown in this section to demonstrate the capacities of the model and the reliability of the approach. The simulation domain dimensions are $1 \times 1 \times 1m$, the mesh is composed of 16×16 elements in the plane (x,y) and 40 elements in the z-direction.

Homogeneous material

The first set of test case is the simulation of the propagation of the electromagnetic field in a homogeneous material. Two material types are simulated: absorbent ($\sigma = 0.03\ \varepsilon = \varepsilon_0, \mu = \mu_0$, ε_0 and μ_0 being the permeability and permittivity of the vacuum) and non-absorbent ($\sigma = 0, \varepsilon = \varepsilon_0, \mu = \mu_0$). The imposed Dirichlet BC are defined by (12). On each side of the domain, tangential components are imposed and normal component is free. The simulation results are presented on **FIGURE 2**. The electric field is depicted in the plane defined by $z = 0.5m$.

$$\boldsymbol{n} \times \boldsymbol{E} = \begin{pmatrix} 0 \\ 0 \\ \sin(\omega\sqrt{\varepsilon\mu}x) \end{pmatrix} \tag{12}$$

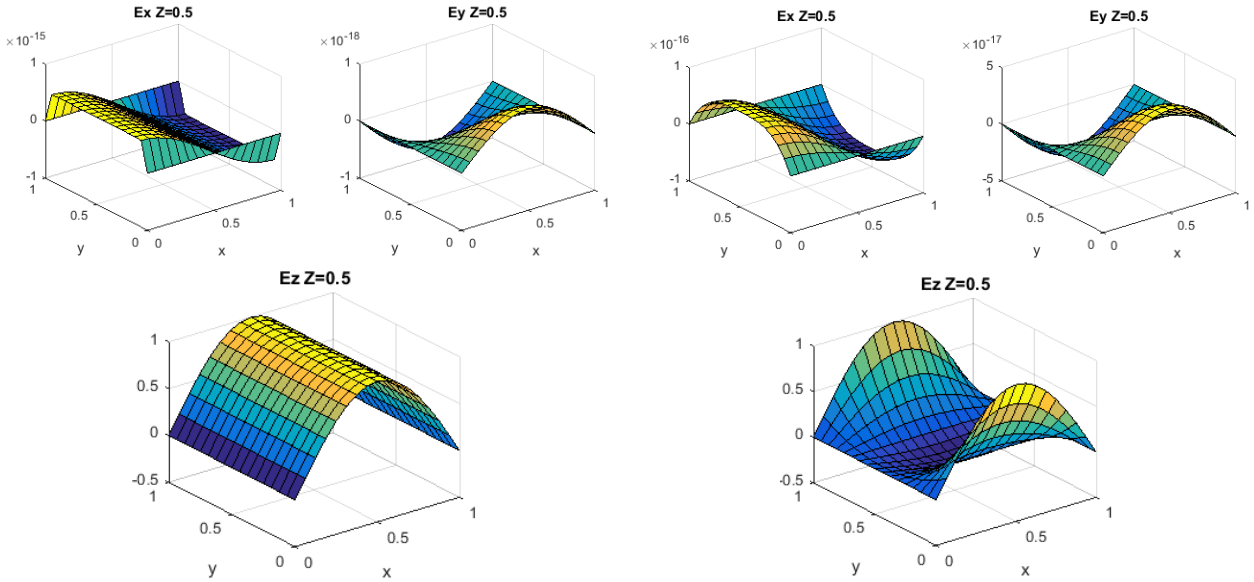

FIGURE 2. PGD simulation results for two homogeneous materials: electric field in non-absorbent (a) and absorbent (b) materials.

The equivalent simulation cases have been performed with 3D Finite Element Method and similar results have been observed. From this comparison, the plane-out-of-plane representation and simulation can be validated. As detailed above, the PGD approach will become crucial when dealing with laminates and shell materials.

2-layer material

The second test case deals with a layered material: field discontinuity has to be enforced at the interface. The simulation case is defined according to **FIGURE 3**.

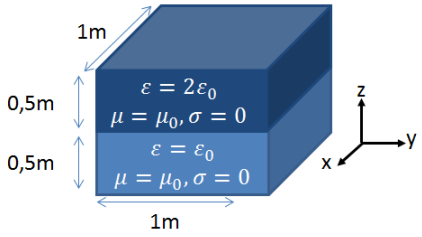

with $\boldsymbol{n} \times \boldsymbol{E} = \begin{pmatrix} y \\ z \\ x \end{pmatrix}$ for the bottom layer

and $\boldsymbol{n} \times \boldsymbol{E} = \begin{pmatrix} y \\ z \\ 2x \end{pmatrix}$ for the top layer as Dirichlet BC

FIGURE 3. Test case definition: bi-layered material with its Dirichlet BC.

Simulation results are given on **FIGURE 4**. The electric field is depicted in the plane z=0.5m, i.e. the interface plane. On the **FIGURE 4a**, the field is $\boldsymbol{E}(z^-)$ in the bottom layer and on **FIGURE 4b**, the field is $\boldsymbol{E}(z^+)$ in the top layer. As expected, the components E_x and E_y are the same because of the continuity of the tangential components. On the contrary, the component E_z shows a discontinuity with the ratio $E_z(z^+)/E_z(z^-) = \varepsilon_{bottom}/\varepsilon_{top} = 1/2$.

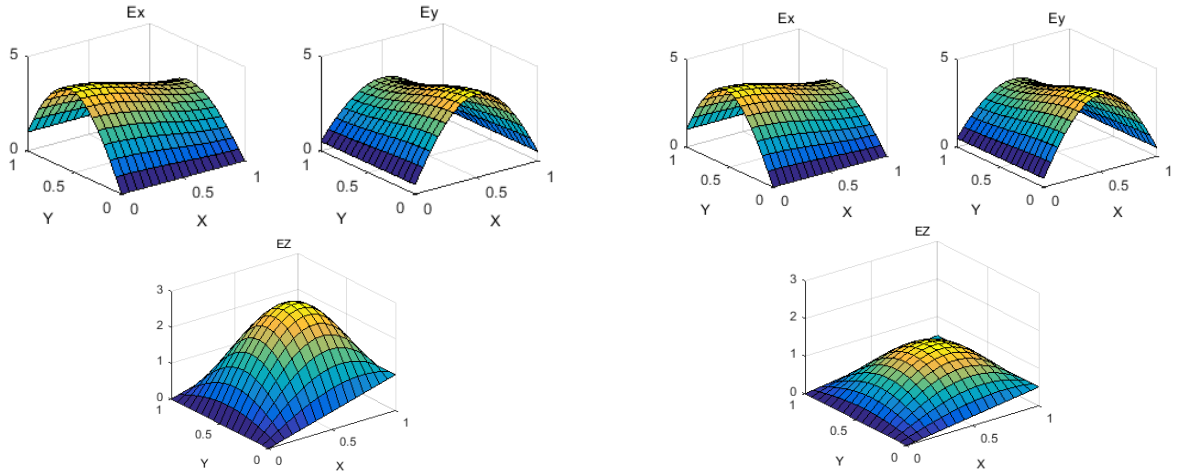

FIGURE 4. PGD simulation results for a 2-layer material: electric field components in bottom layer (a) and in the top layer (b).

CONCLUSION

The modelling of the electromagnetic heating of a GFRP plate has been presented in the paper. First steps of the simulation tool has been detailed and shows that the simulation approach chosen (in-plane-out-of-plane representation within the PGD framework) ensures good results and is able to enforce field representation at interfaces. Further simulation work is to develop the simulation tool to take into account the plies scale in laminates and couple the electromagnetic and thermic physics.

ACKNOWLEDGMENT

This work has been done in the framework of SIMUTOOL project (H2020).

REFERENCES

1. G. Hug, "Behavior analysis of carbon-epoxy laminates under high-speed loading: manufacture of the same materials by means of microwave curing for comparison" Ph.D. thesis, Arts et Métiers ParisTech, 2005.
2. L. Feher, K. Drechsler and J. Pfilsinger, "Composite manufacturing by using a novel modular 2.45 GHz microwave processing system", in *36th International SAMPE Technical Conference*, San Diego, CA, USA. (2004)
3. R. Youssof, M.K. Aroua, A. Nesbitt and R.J. Day, "Curing of polymeric composites using microwave resin transfer moulding (RTM)", in *Journal of Engineering Science and Technology*, **2**(2), 51-163
4. M. Kwak, P. Robinson, A. Bismarck and R. Wise, "Curing of Composite Materials Using the Recently Developed Hephaistos Microwave", in *18th International Conference on Composite Materials*, 21-26 (2011)
5. B. Bognet, A. Leygue, F. Chinesta, A. Poitou and F. Bordeu, "Advanced simulation of models defined in plate geometries: 3D solutions with 2D computational complexity", in *Computer Methods in Applied Mechnanics and Engineering*, **201**, 1-12 (2012)
6. F. Chinesta, A. Leygue, B. Bognet, Ch. Ghnatios, F. Poulhaon, F. Bordeu, A. Barasinski, A. Poitou, S. Chatel and S. Maison-Le-Poec, "First steps towards an advanced simulation of composites manufacturing by automated tape placement" in *International Journal of Material Forming*, **7**(1), 81-92 (2014)
7. Ch. Ghnatios, F. Chinesta and Ch. Binetruy, "3D Modeling of squeeze flows occurring in composite laminates", in *International Journal of Material Forming*, **8**(1), 73-83 (2015)
8. Ch. Ghnatios, E. Abisset-Chavanne, Ch. Binetruy, F. Chinesta and S. Advani, "3D Modeling of Squeeze Flow of Multiaxial Laminates", submitted in *Journal of Non-Newtonian Fluid Mechanics*
9. R. Otin, "Regularized Maxwell Equations and Nodal Finite Elements for Electromagnetic Field Computations" in *Electromagnetics*, **30**(1-2), 190-204 (2010).